JOURNAL OF NATURAL PRODUCTS

pubs.acs.org/jnp

Article

Antinociceptive Benzothiazine and Benzothiazole Natural Products from Marine *Croceibacter atlanticus*

Erin M. Marshall, Chenxi Zhu, Lydia Mayhood, Zain Khalid, Haoyi Yao, Giuliana Panieri, José D. D. Cediel-Becerra, Marc G. Chevrette, James A. Strother, and Sandra Loesgen*

Cite This: *J. Nat. Prod.* 2026, 89, 1265−1275

Read Online

ACCESS | Metrics & More | Article Recommendations | Supporting Information

ABSTRACT: With the goal of identifying new therapeutic leads to treat pain, we screened a library of microbial chemical extracts using the Embryonic Zebrafish Irritant-evoked Hyperlocomotion (EZIH) assay, an *in vivo* phenotypic assay for analgesic/antinociceptive activity. We found that extracts from the bacterium *Croceibacter atlanticus* substantially altered behavioral responses. Using behavior-guided fractionation to identify the active partitions, we determined that the known 1,4-benzothiazin-3-one BPSS2111−2113:C and the new benzothiazole croceithiazole A suppress behavioral responses to painful and/or nociceptive stimuli without apparent acute toxicity. Further investigation with radioligand binding assays revealed that BPSS2111−2113:C shows selective binding to both the serotonin receptor 5-HT2B and the benzodiazepine site of GABAA receptors, while croceithiazole A appears to bind the peripheral benzodiazepine receptor. These results suggest that BPSS2111−2113:C and croceithiazole A are interesting leads as analgesics, sedatives, anesthetics, or molecular probes.

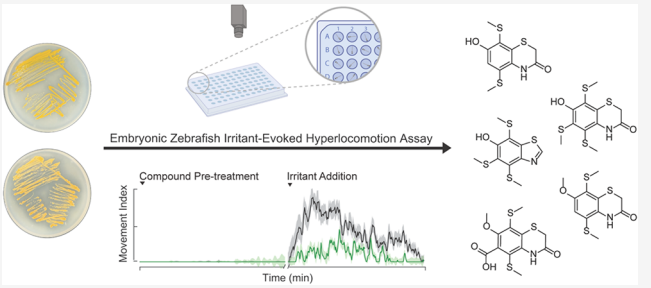

Chronic pain is pain that persists for more than three months, often as a comorbidity of many diseases, including cancer and diabetes.[1] Chronic pain has an outsized impact on human health, affecting 10−40% of humans worldwide, with many individuals reporting that their pain is not managed by typical pain relief medication.[2−4] The factors that contribute to chronic pain are complex and not fully understood, but many forms of chronic pain involve sensitization of nociceptive pathways, which detect tissue damage or noxious stimuli.[5−7] Zebrafish are an excellent model both for studying nociceptive pathways and for the discovery of novel compounds targeting these pathways, since these processes are highly conserved across vertebrate species and zebrafish are amenable to high-throughput strategies. The Embryonic Zebrafish Irritant-evoked Hyperlocomotion (EZIH) assay is a recently developed behavioral model for identifying effects on nociceptive responses.[8] As an *in vivo* approach, the EZIH assay selects for compounds with favorable ADMET properties (absorption, distribution, metabolism, excretion, toxicity) and captures complex interactions that may be lost in *in vitro* methods.[8]

Here, this assay was successfully used to discover a benzothiazole and benzothiazine from the underexplored Gram-negative marine bacterium *Croceibacter atlanticus*, which was first described in 2003 as a new species belonging to the family Flavobacteriaceae.[9] *C. atlanticus* is a ubiquitous marine flavobacterium found in diverse locations from the Arctic and Antarctic Oceans to the Mediterranean and Bering Seas.[10] Previously sequenced *Croceibacter* isolates share high genetic similarity, all belonging to the one named species, *C. atlanticus*. This Gram-negative bacterium has been shown to prevent cell division and metabolism in the diatom *Thalassiosira pseudonana*.[11,12] It has been further implicated in phytoplankton blooms whereas the abundance of *C. atlanticus* increased as the bloom progressed.[13] Other than its association with diatoms, several bacteriophages that infect this marine bacterium have been described.[10,14] To the best of our knowledge, no bioactive secondary metabolites from *C. atlanticus* have been characterized. The 1,4-benzothiazin-3-one class of compounds are rare natural products and are more often reported from synthetic organic chemistry and medicinal chemistry approaches.[15−17] Gram-positive bacteria, such as *Nocardiopsis* sp. and *Streptomyces* sp., produce known 1,4-benzothiazin-3-one containing natural products including nocarterphenyl B, the thiazinotrienomycins, heronamycin A, herbimycin D, thiocarbazomycin A and B, and some geldanamycin derivatives.[18−23] *Burkholderia* sp. has been shown to produce the BPSS2111−2113 family of compounds

Received: January 23, 2026
Revised: April 2, 2026
Accepted: April 3, 2026
Published: April 9, 2026

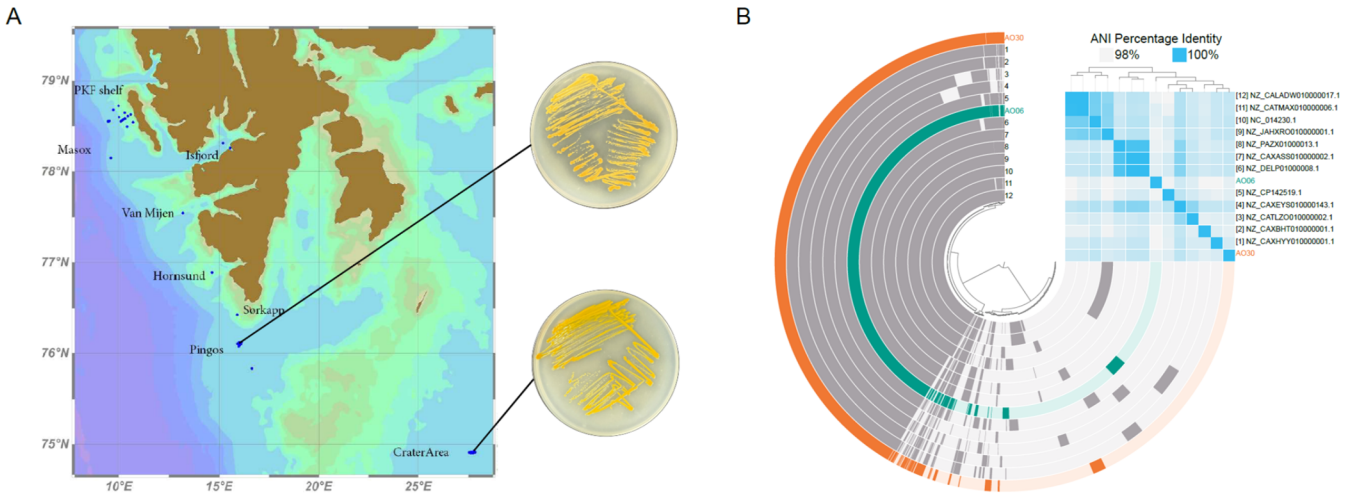

Figure 1. Identification of environmental *C. atlanticus* isolates. (A) Location of environmental sample collection and origin of both *C. atlanticus* isolates. Modified from CAGE 16−5.[31] (B) Avio'o pangenome analysis[34] of public NCBI strains (gray) compared to AO-06 (green) and AO-30 (orange). Average nucleotide identity (ANI) heatmap in the upper right denotes similarity between genomes. Gene content (dark = present, light = absent) is represented in the clock representation. Dendrogram at top right reflects Euclidean clustering of ANI values.[34,35]

via heterologous expression of operons of unknown function,[24,25] and some fungi have been found to produce leptothiazinone A, isocochlioquinone D and its derivatives.[26,27] Beyond microbes, marine macroorganisms including ascidians and tunicates are known for the shermilamine class of benzothiazines.[28,29] These compounds report a range of bioactivity, including antimicrobial, cytotoxic, and immunosuppressant activity.

We show that *C. atlanticus* is a prolific producer of 1,4-benzothiazin-3-one compounds, producing BPSS2111−2113:B (**1**) and BPSS2111−2113:C (**2**) previously only seen from *Burkholderia*, as well as new compounds croceithiazine A (**4**) and croceithiazine B (**5**). We demonstrate antinociceptive activity *in vivo* for benzothiazine BPSS2111−2113:C (**2**), and the newly discovered croceithiazole A (**3**) in our zebrafish model. *In vitro* human receptor binding studies revealed that BPSS2111−2113:C (**2**) shows micromolar affinity for the 5-HT2B serotonin receptor and to the benzodiazepine site of GABAA receptors, while croceithiazole A appears to bind the peripheral benzodiazepine receptor (PBR).

RESULTS AND DISCUSSION

Croceibacter Atlanticus Strain Isolation

Sediment and water samples were supplied from two cruises taken by the Arctic University of Norway (UiT) working with the Centre for Arctic Gas Hydrate, Environment, and Climate (CAGE). The objective of these cruises was to study the geochemistry of the seafloor surrounding the archipelago of Svalbard as there are unique gas-hydrate pingos (GHPs) that consist of large gas-hydrate containing domes. Here, large amounts of gas, including up to 130 mL/L methane, are released into the water column.[30] The first CAGE cruise (16.5) was taken in 2016, and the second cruise (17.2) in 2017.[31,32] The Loesgen Lab was provided with 19 sediment and 30 water samples from both cruises, collected with a remotely operated vehicle (ROV) equipped with a box corer, blade corer, and remotely opened water bottles capable of collecting both sediment and water samples. Two different types of agar plates were used for the isolation of environmental microorganisms: Actinomycete Isolation Agar and Starch Yeast Peptone seawater (SYP-SW) medium. Sediment samples were dried overnight and then stamped onto agar plates using a sterile foam plug. The water samples were plated in a serial dilution. Emerging colonies were further propagated until a monoculture was obtained. The combination of dry stamping of sediment and serial dilution of water samples resulted in the isolation of 85 distinct bacterial isolates.

Bacterium Arctic Ocean 06, henceforth referred to as AO-06, was isolated from a water sample collected at a depth of 4.3 m at the Pingo Location.[31] Isolate Arctic Ocean 30 (AO-30) came from a water sample collected at a depth of 152 m at the Bjørnøyrenna craters (Figure 1A).[31] AO-06 and AO-30 genomes were sequenced using Oxford Nanopore long read technology and identified (via BLAST)[33] as *C. atlanticus*. A pangenome analysis of all deposited full-length *C. atlanticus* genomes revealed an overall average nucleotide identity (ANI) greater than 98%, but showed that AO-06 and AO-30 are distinct strains with some variable gene content (Figure 1B).[34,35] *C. atlanticus* isolates AO-06 and AO-30 were selected for further analysis as no secondary metabolites have previously been reported from this genus, and the microbial extracts proved to be chemically rich by chromatographic analysis.

Compound Isolation and Structure Determination

Both AO-06 and AO-30 isolates were grown in tyrosine and methionine-supplemented marine media prior to absorption onto XAD-7 resin and subsequent extraction with methanol and acetone. Organic extracts were dried under reduced pressure and re-extracted with 1:1 ethyl acetate and water. The extracts were further fractionated via reverse-phase preparative HPLC prior to compound isolation with reverse-phase analytical high-performance liquid chromatography (HPLC).

Compound **1**, a pale yellow solid, was isolated via semipreparative reverse-phase HPLC using a gradient of 20−60% acetonitrile, where ultraviolet (UV) was monitored at 240 and 280 nm for compound collection. High resolution mass spectrometry (HRMS) analysis of compound **1** resulted in *m/z* values of 274.0033 $[M + H]^+$ and *m/z* 271.9873 $[M\text{-}H]^-$, consistent with the molecular formula of $C_{10}H_{11}NO_2S_3$ and six degrees of unsaturation (Figure S2). The compound had a

https://doi.org/10.1021/acs.jnatprod.6c00098
J. Nat. Prod. 2026, 89, 1265−1275

unique UV profile, with absorbances at <200, 264, and 320 nm (Figure S1). ^{1}H nuclear magnetic resonance (^{1}H NMR) revealed two methyl singlets (δ_H 2.30 and 2.46), and singlets each for methylene (δ_H 3.41), methine (δ_H 6.77), hydroxyl (δ_H 6.91), and amine (δ_H 7.95) groups. ^{13}C NMR showed ten carbon signals, consistent with the proposed molecular formula (δ_C 17.6, 18.4, 30.7, 113.7, 116.8, 128.9, 129.06, 129.10, 153.7, and 164.2). Heteronuclear single quantum coherence (HSQC) correlations connected four carbon atoms to their respective hydrogen atoms, two of which are methyl groups, and heteronuclear multiple bond correlation (HMBC) established the connection of fragments (Figure 2, S3−S9). The thiomethyl groups exert strong shielding effects on the ^{1}H and ^{13}C chemical shifts as expected (Table 1).

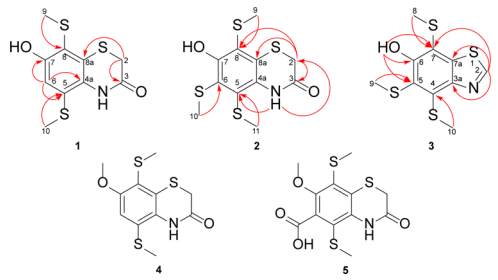

Figure 2. Key HMBC correlations (red arrows) for compounds **1**-**3**. Proposed structures of croceithiazine A (**4**) and croceithiazine B (**5**).

Compound **2** was similarly isolated using a gradient of 30−70% acetonitrile. **2** is a yellow powder and ionized with m/z values of 319.9911 $[M + H]^+$ and m/z of 317.9758 $[M-H]^-$, consistent with the molecular formula of $C_{11}H_{13}NO_2S_4$ and six degrees of unsaturation (Figure S10). Its UV profile had similar absorbance maxima at 200, 266, and 346 nm compared to **1**, indicative of a similar scaffold (Figure S1). ^{1}H NMR data consisted of three methyl singlets (δ_H 2.37, 2.40, and 2.40), and singlets for methylene (δ_H 3.43), hydroxyl (δ_H 7.47), and amine (δ_H 8.70) groups. ^{13}C NMR supported the molecular formula with 11 carbon resonances (δ_C 17.9, 19.7, 19.7, 30.6, 120.7, 125.1, 129.4, 129.5, 132.0, 154.6, and 164.4). HSQC correlations were used to identify one methylene and three methyl groups (Figures 2, S11−S16).

Compounds **1** and **2** were determined to be BPSS2111−2113:B and BPSS2111−2113:C respectively by comparison to published NMR and MS data from Biggins et al.[24] Our analyses encountered the same reported issues with chemical shift assignment, where C4a, C8a, and C8 of BPSS2111−2113:B have very similar chemical shifts and were previously noted as interchangeable. For **1**, these carbon signals (δ_C = 128.9, 129.06, 129.10) were very close to each other and difficult to resolve in 2D spectra. Heteronuclear multiple bond correlation (HMBC) data exhibited correlations from these three carbons to δ_H values of 2.46 (H-9), 3.41 (H-2), and 6.91 (H-6). The δ_C 128.9 has a distinct correlation to δ_H 6.91 (H-6) and was assigned as C4a. C8 and C8a were more difficult to resolve with their similar chemical shifts (δ_C = 129.06 and 129.10). However, we were able to connect 3.41 (H-2) to δ_C 129.06 and δ_H 2.46 (H-9) to δ_C 129.10 using HMBC correlations (8 Hz) leading to the assignment of C8 at δ_C 129.10 and C8a at δ_C 129.06 (Figure S8).

Similarly, the published NMR assignments for C6 and C8 as well as C9 and C10 in BPSS2111−2113:C (**2**) were noted as interchangeable. HMBC showed correlations between H-2 and C8, which determined the correct chemical shifts of C6 and C8 and their corresponding thiomethyl groups (Figure S15), adding more structural information to the previous assignments for both BPSS2111−2113:B and:C.

Compound **3** was isolated as a yellow-brown powder via semipreparative HPLC using a gradient of 40−80% acetonitrile. **3** was found to have an m/z value of 287.9657 $[M-H]^-$ with a molecular formula of $C_{10}H_{11}NOS_4$ (Figure S17). The UV absorbances at 200, 240, 270, and 322 nm did not indicate a benzothiazine core (Figure S1), but the isotopic pattern supported the presence of four predicted sulfur atoms from the accurate mass derived formula. NMR analyses, including long-range heteronuclear single quantum multiple bond correlation (HSQMBC), allowed characterization of this compound.[37] ^{1}H NMR revealed three methyl groups (δ_H 2.39, 2.48, 2.84), one hydroxyl (δ_H 7.79), and a methine (δ_H 8.86). ^{13}C NMR, supported by 2D techniques, revealed ten carbon atoms (δ_C

Table 1. ^{1}H and ^{13}C NMR Spectroscopic Data for Compounds 1, 2, and 3, 600 MHz, Dichloromethane-d_2, Cryoprobe, 1.7 mm Tubes

	BPSS2111−2113:B (**1**)		BPSS2111−2113:C (**2**)		Croceithiazole A (**3**)	
Position	δ_C, type	δ_H	δ_C, type	δ_H	δ_C, type	δ_H
2	30.7, CH_2	3.41, s	30.6, CH_2	3.43, s	151.9, CH	8.86, s
3	164.2, C		164.4, C			
3a					144.1, C	
4					140.2, C	
4a	128.9, C		132.0, C			
5	116.8, C		129.4, C		123.0, C	
6	113.7, CH	6.91, s	125.1, C		155.7, C	
7	153.7, C		154.6, C		111.2, C	
7a					146.8, C	
8	129.10, C		120.7, C		17.6, CH_3	2.48, s
8a	129.06, C		129.5, C			
9	17.6, CH_3	2.46, s	19.7, CH_3	2.40, s	19.2, CH_3	2.39, s
10	18.4, CH_3	2.30, s	17.9, CH_3	2.40, s	20.1, CH_3	2.84, s
11			19.9, CH_3	2.37, s		
NH		7.96, s		8.70, s		
OH		6.77, br. s		7.47, br. s		7.79, s

https://doi.org/10.1021/acs.jnatprod.6c00098
J. Nat. Prod. 2026, 89, 1265−1275

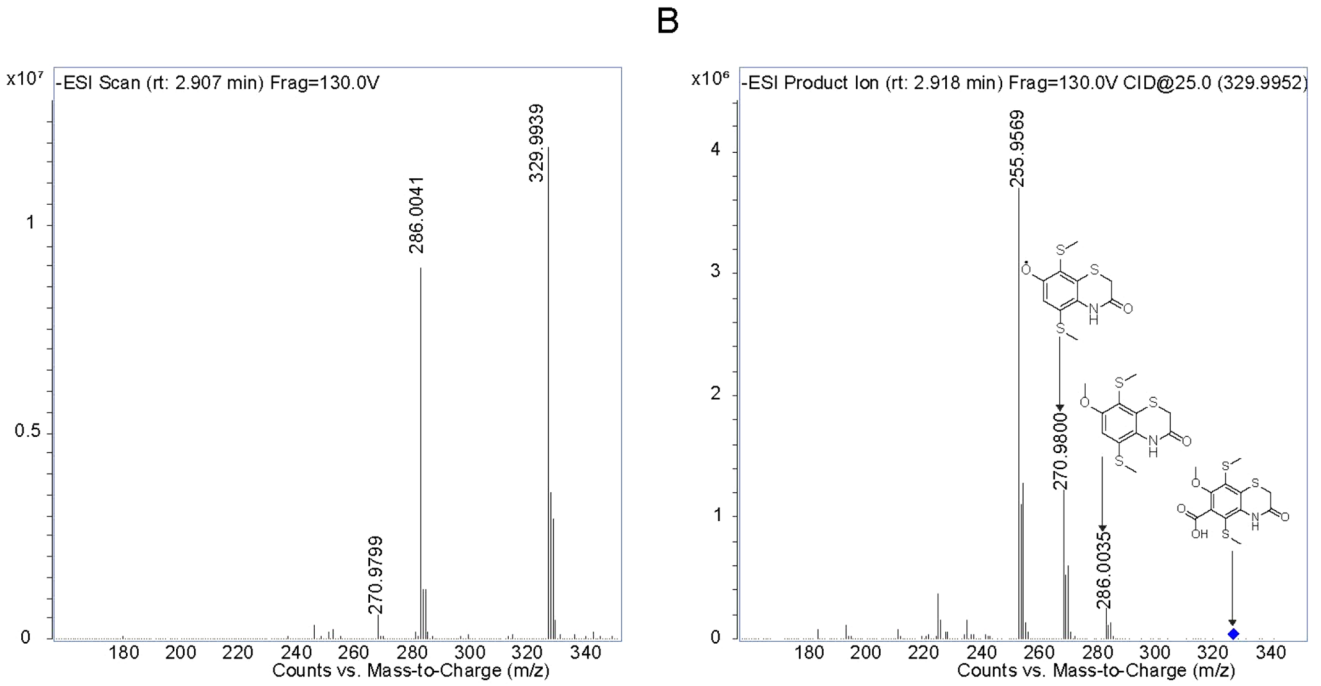

Figure 3. HRMS-based characterization of croceithiazine A (**4**) and croceithiazine B (**5**). (A) HRMS spectrum showing masses for proposed compounds **4** (*m*/*z* 286.0041) and **5** (*m*/*z* 329.9939). (B) Annotated MS^2 spectrum of **5**, revealing fragmentation into masses indicating compounds **4** and **1** (*m*/*z* 270.9800).

17.6, 19.7, 20.1, 11.2, 123.0, 140.2, 144.1, 146.8, 151.9, 155.7). Both 8 and 12 Hz filtered HMBC spectra were used to find correlations between the hydroxyl and neighboring carbons, which were not found in the 4 Hz filtered HMBC. This compound was determined to be a new benzothiazole with substituents on the benzene ring similar to those of **2** (Figures 2, S18−S27).

Two more compounds were isolated via preparative HPLC using the same gradient as that for **1**. HRMS analysis revealed a *m*/*z* value of 286.0038 $[M\text{-}H]^-$ for **4** and a *m*/*z* value of 329.9930 $[M\text{-}H]^-$ for **5**. The UV absorbances for both were at 200, 258, and 332 nm and matched the benzothiazine profile of **1**. In addition, **5** can be fragmented in MS/MS (-ESI) into *m*/*z* features of 286.0030 and 270.9806, corresponding to the accurate masses of **4** and **1**, respectively (Figure 3). For both compounds **4** and **5**, we propose an additional methoxy group based on the mass increase of 15.024u as quantified by HRMS/MS. Further, the mass difference of 43.992u between **4** and **5** indicates the presence of a carboxylic acid group in **5**, which is lost in **4**. We propose the names croceithiazine A and croceithiazine B for **4** and **5**, respectively.

Identification of Antinociceptive Metabolites *In Vivo*

The zebrafish-based EZIH assay was utilized to evaluate any nociceptive effects of these compounds.[8,37] Briefly, embryonic zebrafish are pretreated with a test compound and then exposed to a noxious chemical stimulus (allyl isothiocyanate [AITC], a TrpA1 agonist), and the locomotor responses are recorded. In untreated animals, AITC elicits a robust hyperlocomotion response. Pretreatment with analgesic compounds (e.g., lidocaine, buprenorphine, HC-030031) significantly reduces this hyperlocomotion response, while pretreatment with compounds that do not have established antinociceptive properties does not alter the response. Following the assay, animals are observed under a microscope for morphological or cardiac changes suggestive of acute toxicity. Single-dose responses were compared against vehicle saline trials using a two-sample, two-tailed *t* test. Dose response curves were analyzed using a one-way ANOVA with posthoc pairwise comparisons (*p*-values are reported for the ANOVA and/or the most relevant pairwise comparison). The concentration dependence of observed effects was then quantified by computing the $\log_{10}$EC50 by fitting responses to the Hill Equation and estimating the standard error of the mean (S.E.M.) using a bootstrap analysis.

In preliminary screens of the extract and preparative HPLC fractions, activity was found in fractions containing **1**, **2**, **3**, **4**, and **5**. Isolated pure compounds were tested in the EZIH assay at a final concentration of 40 μM, which revealed that **2** and **3** exhibited decreased nociceptive responses compared to saline controls. Compounds **1**, **4**, and **5** did not appear to alter nociceptive responses (Figure S29). None of the compounds produced signs of acute toxicity. A comparison of the active and inactive metabolites suggests that the third thiomethyl group of **2** and **3** must be present for activity. Compounds **1** and **4** are lacking this group, while **5** is potentially blocks access to this position with the bulky carboxylic acid moiety. Dose response assays were then performed on the active metabolites, and **2** exhibited an *in vivo* EC_{50} of 17.0 μM (Figure 4 A-B; p = 0.01 for ANOVA; p = 0.061 for 0 μM vs 80 μM; $\log_{10}$EC50: −4.77 ± 0.35 [M], mean ± S.E.M.) and **3** yielded an EC_{50} of 40.6 μM (Figure 4 C−D; $p < 0.0001$ for ANOVA; $p < 0.0001$ for 0 μM vs 60 μM; $\log_{10}EC_{50}$: −4.39 ± 0.06 [M], mean ± S.E.M.). Notably, **2** shows increased potency compared to **3**, but **3** shows increased efficacy.

Compounds **1**−**5** were additionally tested in a single dose assay (10 mg/mL) against *Staphylococcus aureus* (ATCC 25923), *Escherichia coli* (ATCC 8739), and *Candida albicans* (ATCC 90027) and exhibited no activity.[38−40] In addition, compounds showed no activity in 3-(4,5-dimethylthiazol-2-yl)-

https://doi.org/10.1021/acs.jnatprod.6c00098
J. Nat. Prod. 2026, 89, 1265−1275

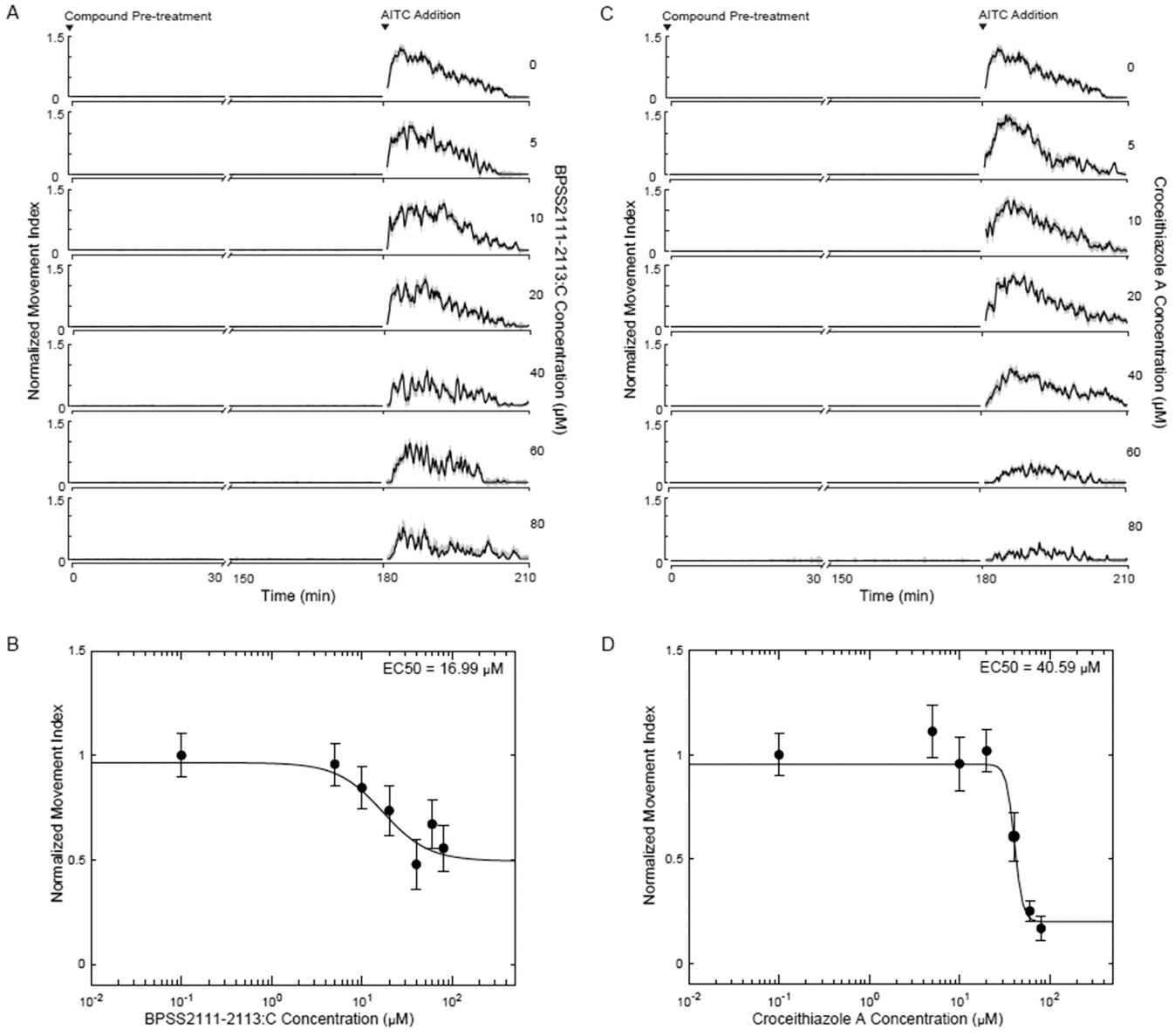

Figure 4. Antinociceptive activity of **2** and **3** in the zebrafish EZIH assay. (A) Time series showing locomotor activity throughout EZIH assay following pretreatment with varying concentrations of **2**, from 0 (top) to 80 μM (bottom) (N = 12; median ± S.E.M.). (B) Dose response curve for **2** showing effects on behavioral response to nociceptive stimulus (average locomotor activity for period 1−6 min after AITC addition, N = 12 each, shown as median ± SEM across trials, 0 μM plotted at 0.1 μM). (C) Similar to A, showing time series of locomotor activity following pretreatment with **3**, from 0 (top) to 80 μM (bottom). (D) Similar to B, showing a dose response curve for **3**.

2,5-diphenyltetrazolium bromide (MTT) mammalian cell viability assays when tested at 10 μM.[41]

Mode of Action Determination

Motivated by the observed activity in EZIH assays, **2** and **3** were submitted to the NIH Psychoactive Drug Screening Program (PDSP). This program enables high-throughput testing for activity against a wide range of G-protein-coupled receptors.[42,43] Binding assessment was performed as a radioligand competition assay as per the PDSP protocol. Single-dose binding assessment suggested that **2** exhibits selective binding to the benzodiazepine (BZP) site of GABAA and the 5-HT2B G-protein-coupled receptor (GPCR) (Figure 5A). Subsequent dose response assays indicated that **2** shows a binding affinity (K_i) of 1.18 μM to the BZP site and 2.23 μM to the 5-HT2B receptor (Figure S30). Similarly, single-dose assays suggested that **3** may exhibit effects at the peripheral benzodiazepine receptor (PBR), and some binding to the sigma-1 receptor (Figure 5B). Further testing of this mechanism of action is ongoing. While the binding profiles of BPSS2111−2113:C and croceithiazole A differ, both seem to affect benzodiazepine related targets and warrant further exploration.

Biosynthetic Origin

C. atlanticus, a marine flavobacterium, produces the same compounds discovered via genome mining from *Burkholderia pseudomallei* and isolated from a trimethoprim-resistant human pathogenic*Burkholderia* sp., associated with cystic fibrosis. McAvoy et al.[25] suggested a biosynthetic route for production of BPSS2111−2113:B involving the biosynthesis of homogentisic acid and subsequent amino acid-mediated modification, followed by methylthiolation and oxidative removal of the side chain (Figure 6). Homogentisic acid production via the

https://doi.org/10.1021/acs.jnatprod.6c00098
J. Nat. Prod. 2026, 89, 1265−1275

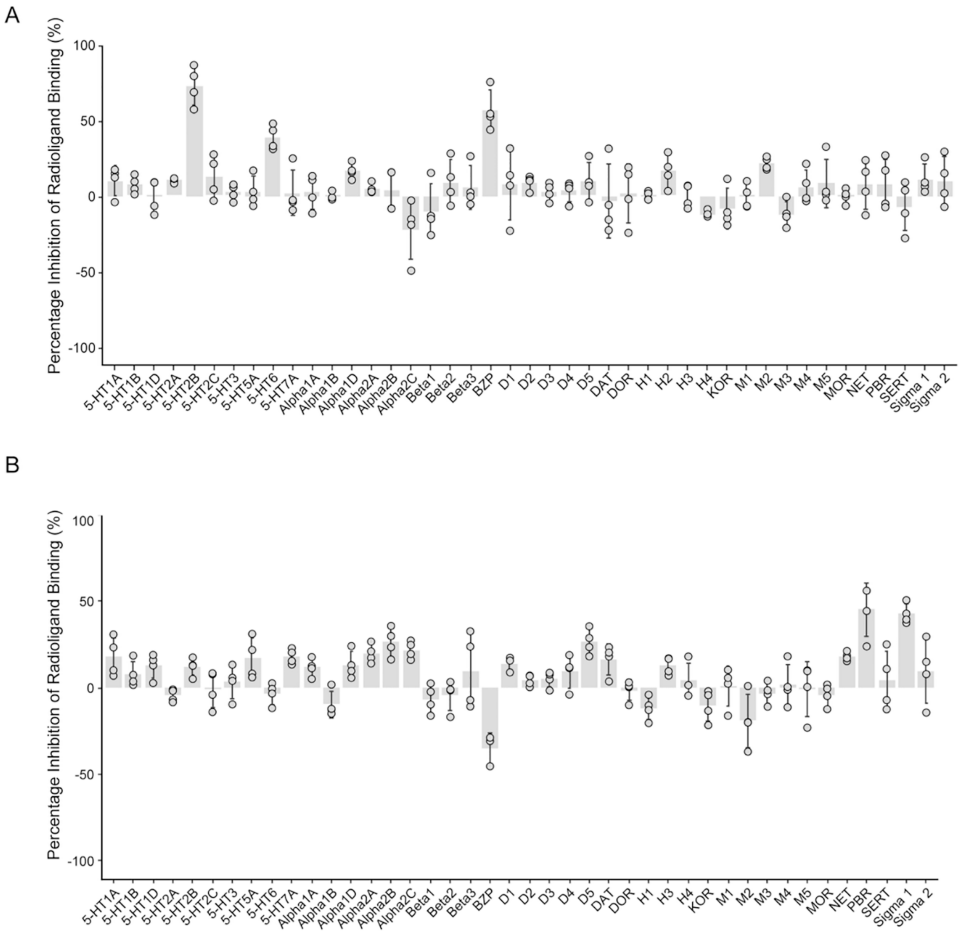

Figure 5. NIH PDSP human receptor binding assessment. Percent inhibition of radioligand binding by **2** (A) and **3** (B) against human GPCR was observed for four trials.

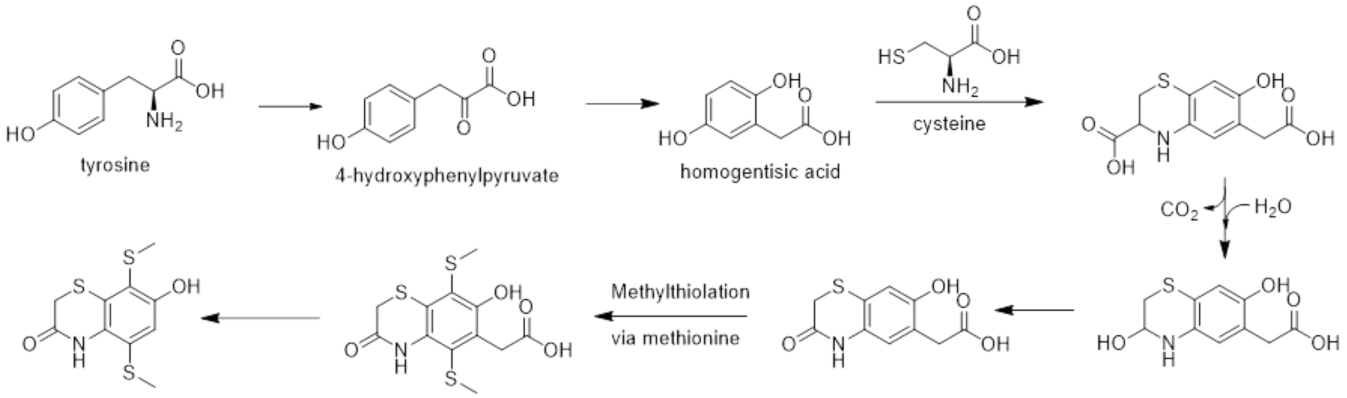

Figure 6. Predicted biosynthesis of BPSS2111−2113:B. Reproduced and modified from [25]. Copyright 2023 American Chemical Society.

enzymatic metabolism of tyrosine is well documented.[44,45] As homogentisic acid was not isolated from *C. atlanticus* extractions but is present in the predicted biosynthetic pathway for production of BPSS2111−2113:B,[25] we probed the genome for these enzymes. In this pathway, tyrosine is converted to 4-hydroxyphenylpyruvate by a tyrosine aminotransferase, followed by conversion into homogentisic acid by 4-hydroxyphenyl-pyruvate dioxygenase. We identified a gene with 35% sequence identity to 4-hydroxyphenylpyruvic acid dioxygenase (*WP_038759037.1*) in both AO-06 and AO-30 genomes. Gene neighborhood analysis by GATOR-GC[46] further revealed additional genes with known involvement in the homogentisate biosynthetic pathway including homogentisate 1,2-dioxygenase.

BPSS2111−2113:B and :C were first discovered via the heterologous expression of *B. pseudomallei* cryptic operons BPSS2111−2113. However, it was determined that the expression of BPSS2111 alone produced these products. BPSS2111, predicted to be an FAD-dependent monooxygenase, was postulated to produce the benzothiazine core, and it was suggested that host enzymes were responsible for the thiomethyl additions.[24] Due to the rarity of natural product

https://doi.org/10.1021/acs.jnatprod.6c00098
J. Nat. Prod. 2026, 89, 1265−1275

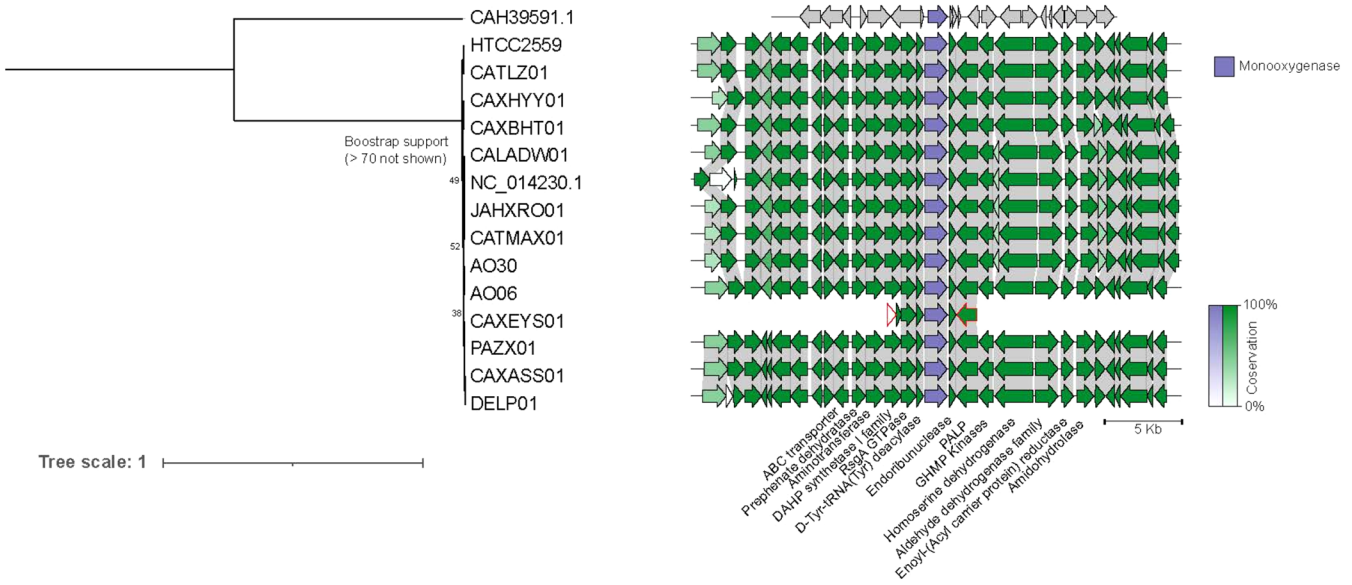

Figure 7. Conservation of the monooxygenase encoding gene and gene neighborhoods postulated to be involved in the biosynthesis of benzothiazines. Genomes other than AO-06 and AO-30 were sourced from the NCBI. GATOR-GC gene neighborhoods denote relative opacity of genes, which represents percent conservation across all *C. atlanticus* genomes. The monooxygenase is shown in purple, and contig edges are shown as red outlines.

benzothiazines, we hypothesized that both *C. atlanticus* and *B. pseudomallei* may contain the same genes needed for production of BPSS2111−2113:B and :C. The *Burkholderia* gene region BPSS2111 was compared to the full genomes of AO-06 and AO-30 (tBLASTn), where one region of interest was identified as matching by ∼ 22% sequence identity. These predicted enzymes are almost identical between AO-06 and AO-30, with one amino acid substitution, and were predicted to function as monooxygenases.

To investigate evolutionary relationships, we constructed a phylogenetic tree based on the monooxygenase sequence of the environmental *C. atlanticus* strains as compared to the other NCBI submitted *C. atlanticus* isolates, using the *B. pseudomallei* monooxygenase (CAH39591.1) as an outgroup (Figure 7). The *C. atlanticus* monooxygenase forms a distinct clade separate from *B. pseudomallei*. Relative opacity of the genes indicates gene conservation among the *C. atlanticus* isolates, revealing that these genes are highly conserved in the genus. Oxidative benzothiazine production seems to be unique in *C. atlanticus* compared to *B. pseudomallei* and preserved within the *C. atlanticus* genus.

In conclusion, *C. atlanticus* produces unique sulfur-containing specialized metabolites, including those containing the rare 1,4-benzothiazin-3-one scaffold. To our knowledge, these are the first natural products isolated from this genus. Genome mining efforts for biosynthetic gene clusters were unsuccessful, a strong reminder that many marine Gram-negative bacteria are still underrepresented in genomic and chemical exploration. The lack of "classic" natural product biosynthetic gene clusters limits the prediction power of bioinformatic tools like antiSMASH and opens up new avenues for metabolite and biosynthetic discovery.[47,48] While the biosynthesis remains to be experimentally validated, a solid hypothesis has emerged based on our and previous work involving amino acid-modifying enzymes. It is astonishing to find Arctic Ocean derived *Croceibacter* produce the same sulfur-containing small molecules that are made by *Burkholderia* strains associated with human lung disease, specifically with highly virulent and hard-to-treat antibiotic-resistant strains.[25] Indeed, *Croceibacter* was found to be resistant to several antibiotics including but not limited to trimethoprim, ampicillin, kanamycin, and streptomycin in our experiments (data not shown) and the original strain report.[9] The zebrafish-based EZIH assay was instrumental to the identification of the neuroactive effects of the known BPSS2111−2113:C benzothiazine and the new croceithiazole A. Initial testing by the NIH Psychoactive Drug Screening Program using human receptors *in vitro* showed binding affinity of **2** to serotonin receptor 5-HT2B (2.2 μM) and the benzodiazepine site of GABAA (1.2 μM), while preliminary tests indicate that croceithiazole A (**3**) may bind to the peripheral benzodiazepine receptor. Future studies examining the effects of these compounds on receptor responses and neural activity will yield an even deeper understanding of their modes of action. Our findings highlight the potential of unexplored Gram-negative bacteria as a chemically rich source of unique compounds and show the utility of the EZIH assay in the detection of neuroactive compounds from complex mixtures.

EXPERIMENTAL SECTION

General Experimental Methods

Low-resolution ESI-MS was recorded on an Agilent 1100 series LC with an MSD 6130 using a Phenomenex Kinetex C18, 5u 150 mm × 4.0 mm HPLC column. Standard gradient method used ultrapure water (A) and LCMS acetonitrile (B) with 0.05% formic acid. Method involved a 10−100% B gradient over 33 min at a flow rate of 0.8 mL/min. MS parameters for + ESI: 350 °C drying gas temperature, 40 PSI nebulizer pressure, and a 3500 V capillary voltage. MS parameters for -ESI: 275 °C drying gas temperature, 40 PSI nebulizer pressure, and 4000 V capillary voltage.

High-resolution ESI-MS-QTOF spectra were obtained on an Agilent 6546 instrument. Standard gradient method used ultrapure water (A) and LCMS acetonitrile (B) with an additional 0.05% formic acid addition for + ESI only. Method involved a 10−95% B gradient over 9.75 min at 40 °C. The column used was a Phenomenex Kinetex 2.5 μm C18, 50 × 2.1 mm column with a flow rate of 0.4 mL/min. MS parameters for + ESI: 350 °C drying gas temperature, 40 PSI

https://doi.org/10.1021/acs.jnatprod.6c00098
J. Nat. Prod. 2026, 89, 1265−1275

nebulizer pressure, and 3000 V capillary voltage. MS parameters for -ESI: 350 °C drying gas temperature, 40 PSI nebulizer pressure, and 4000 V capillary voltage.

Agilent 1100 series and 1260 Infinity II HPLC systems were used for analytical, semipreparative, and preparative separations, all equipped with photodiode array detectors. Analytical and semi-preparative HPLC used ultrapure water (A) and HPLC acetonitrile (B) with no formic acid addition. The column used was a Phenomenex Luna C18(2), 5u 250 mm × 10 mm column. Methods involved gradients of increasing polarity depending on the compound, and fractions were lyophilized. Preparative HPLC was done on a Luna 5u C18(2) AXIA, 250 mm × 21.2 mm column. This method used ultrapure water (A) and HPLC methanol (B) with no formic acid addition. The method involved a 10−100% B gradient over 55 min at a flow rate of 20 mL/min. Fractions were collected in increments of 10 mL or 0.5 min. Fractions were consolidated and reduced under pressure prior to lyophilization.

NMR data were collected with assistance from AMRIS. Instrument used was a Bruker Avance Neo-600 Console equipped with a Magnex 14.1 T/54 mm AS Magnet and 1.7 mm TCI CryoProbe. All compounds were reconstituted in dichloromethane-d_2.

Bacterial Strain Isolation, Cultivation, and Extraction

Water and sediment samples provided by a UiT CAGE were shipped in sterile containers. Solid agar plates used were Actinomycete Isolation Agar (2 g/L sodium caseinate, 0.1 g/L L-asparagine, 4 g/L sodium propionate, 0.5 g/L dipotassium phosphate, 0.1 g/L magnesium sulfate, 0.001 g/L ferrous sulfate, 15.0 g/L agar, 35.7 g/L Instant Ocean Sea Salt, hydrated in DI water with 0.5% glycerol) and Starch Yeast Peptone seawater (SYP-SW) medium (10 g/L starch, 4 g/L yeast, 2 g/L peptone, 33.3 g/L Instant Ocean Sea Salt, 15 g/L agar with added antifungals: 10 ng/mL nystatin and 10 ng/mL cycloheximide). Water samples underwent serial dilution and were grown on solid media. Sediment samples were either dried overnight and dry stamped onto solid agar or suspended in sterile seawater used to inoculate solid agar. Resulting isolation plates were kept at both 4 and 28 °C to allow for microbial growth. Single strains from these agar plates were then sequentially cultured until a pure isolate remained.

C. atlanticus was cultured on solid media at 28 °C and in liquid media at room temperature, orbitally shaking at 180 rpm. Maintenance of the isolate was cultured on SYP-SW media. For increased production of sulfur-containing compounds, Starch Yeast Peptone seawater media with supplemented tyrosine and methionine (SYP-SW-MY) was used (10 g/L starch, 4 g/L yeast, 1 g/L peptone, 0.5 g/L methionine, 0.5 g/L tyrosine, 33.3 g/L Instant Ocean Sea Salt, 15 g/L agar).

Cultures of all *C. atlanticus* isolates were maintained on SYP-SW agar at 28 °C. A 1 cm^2 section of living culture originating from an agar plate was used to inoculate 100−500 mL of SYP-SW or SYPSW-MY liquid media in an unbaffled flask. These cultures were used to inoculate 1−1.5 L of the respective media and were subsequently incubated at room temperature for 4 weeks, orbitally shaking at 180 rpm. Amberlite XAD-7 (ThermoFisher) was conditioned by hydration in acetone, followed by methanol, and finally ultrapure water. 50−70 g of conditioned resin was added to each large 1−1.5 L culture and was allowed to incubate overnight with shaking. The resin-culture media were filtered through cheesecloth to isolate the resin. The cheesecloth was then tied to contain the resin inside and extracted with an excess of methanol and acetone via sonication for 20 min each. The organic extracts were then reduced under pressure to obtain dry microbial extracts. Upon indication of oxidation, 5 μg of butylated hydroxytoluene (BHT) was added prior to drying the extracts to prevent oxygenation.

Bioactivity Assays

Antimicrobial Assay. Microbial extracts and fractions solubilized in DMSO were tested for antibacterial activity following established protocols in duplicate at a final concentration of 125 μg/mL.[38−40] Antibacterial activity was tested against *Staphylococcus aureus* (ATCC 25923), *Pseudomonas aeruginosa* (ATCC 15442), and *Escherichia coli* (ATCC 8739), and antifungal activity was tested against *Candida albicans* (ATCC 90027), all provided by the American Type Culture Collection (ATCC, Manassas, VA). Reference antibiotics used as positive controls in these experiments were kanamycin (*S. aureus* and *P. aeruginosa*, 50 μg), ampicillin (*E. coli*, 50 μg), and amphotericin B (*C. albicans*, 25 μg). Turbidity was measured by absorbance at 620 nm using a Biotek Synergy reader.

Cell Viability Assay. Microbial extracts and fractions were tested for antimetabolic activity at a final concentration of 10 μg/mL against human colorectal carcinoma mammalian cells (ATCC CCL-247, Manassas, VA) following established protocols.[41] HCT-116 mammalian cells were cultured in Dulbecco's modified Eagle's medium (DMEM) supplemented with 10% (v/v) fetal bovine serum (FBS) and 1X penicillin-streptomycin. Cells were maintained in a humidified incubator at 37 °C with 5% CO_2. HCT-116 cells were seeded in 96-well plates at a density of 7000 cells/well and maintained for 24 h to allow for adherence. Microbial extracts and fractions solubilized in DMSO were added to duplicate wells at a final concentration of 10 μg/mL and incubated for 46 h. MTT ([3-(4,5-dimethylthiazolyl-2)-2,5-diphenyltetrazolium bromide]) solubilized in PBS was added to all wells at a final concentration of 0.5 mg/mL. After two h, the DMEM was removed from the well plate, revealing the purple formazan product formed by the reduction of MTT by metabolically active cells. The formazan crystals were solubilized in 50 μL of DMSO and absorbance was measured at 550 nm. Metabolic activity of 0.5% DMSO treated cells was defined at 100% cell viability, and 10 μM mensacarcin was used as the positive, cytotoxic control. Microbial extracts and fractions that reduced cell metabolism to 60% or less were defined as inhibiting cell viability.

Embryonic Zebrafish Irritant-Evoked Hyperlocomotion Assay (EZIH). *In vivo* activity was measured through the Embryonic Zebrafish Irritant-evoked Hyperlocomotion assay.[8] Briefly, zebrafish larvae aged 52−60 h postfertilization were individually placed into a 96-well plate with HEPES-buffered E3 saline. The test compounds were added to the wells at a final concentration of 25 μg/mL for extracts and fractions, and the response was measured for 30 min to determine the acute effects of the compounds. After an additional two h incubation period, the response was again recorded for 30 min to establish a new baseline and determine the persistent effects of the test compounds. Finally, the TRPA1 agonist allyl isothiocyanate (AITC, mustard oil) was added to the wells at a final concentration of 35 μM, and the response was measured for 30 min. At this age, the larvae have not yet inflated their swim bladders and did not display spontaneous locomotor activity. The addition of a noxious stimulus (such as AITC) causes a tail-flick response that propels the larvae around the wells, which is recorded using a camera above the well plate. Locomotor activity is reported as the normalized movement index, which is the movement index normalized by the same index in animals treated with vehicle saline.

DNA Sequencing. Both environmental isolates of *C. atlanticus* were grown in 5 mL of SYP-SW liquid culture until turbid. Cells were centrifuged at 3000 rpm for 10 min, and the liquid media was removed. Cells were frozen at −80 °C prior to mechanical crushing, which was then resuspended in TE buffer supplemented with lysozyme (20 mg/mL) and incubated for up to an hour at 37 °C. Proteinase K (20 mg/mL) and SDS (10% w/v) were then added, and again the mixture was incubated at 55 °C. After cooling to room temperature, the mixture was extracted with phenol:chloroform (1:1) for up to 10 min prior to centrifugation at 14,000 rpm for 10 min. The aqueous layer was isolated, and 3 M sodium acetate (10% v/v) and isopropanol were added to incite DNA precipitation. DNA was subsequently isolated via centrifugation. DNA was assessed for purity by 260/280 assessment via nanodrop and was quantified by Qbit prior to submission to SeqCenter for nanopore sequencing.

Bacterial Pangenome Analysis. The gene content of the AO-06/AO-30 and *Croceibacter* genomes available in NCBI as of September 2024 was identified and visualized in Anvi'o[34] using the pangenome pipeline.[35] Average Nucleotide Identity (ANI) was calculated with the anvi- compute-genome-similarity module using pyANI. Both genomes and genes were clustered using Euclidean

https://doi.org/10.1021/acs.jnatprod.6c00098
J. Nat. Prod. 2026, 89, 1265−1275

distance, with genomes arranged by ANI percentage identity and genes by presence/absence patterns.[36]

Phylogeny and Gene Cluster Analysis. Phylogenetic analysis of the monooxygenase enzyme from the AO-06/AO-30 and *Croceibacter* genomes (NCBI) was performed using IQ-TREE 2.[49] Maximum Likelihood inference was conducted with the best-fit evolutionary model, and 100 bootstrap replicates were calculated. The monooxygenase from *B. pseudomallei* K96243 (CAH39591.1) was used as an outgroup to root the phylogeny. The phylogenetic tree was visualized and edited using iTOL.[50] Gene clusters were identified using GATOR-GC,[46] with the monooxygenase (*WP_272973609.1*) designated as the required protein. Default parameters were applied for the required distance and window extension. These gene clusters were annotated by using Hidden Markov Model (HMM) profiles from the PFAM database.

■ ASSOCIATED CONTENT

Data Availability Statement

The NMR data for compounds **1**–**3** have been deposited to NP-MRD (https://np-mrd.org) under NP-CARD: NP0353870 (**1**), NP0353871 (**2**), and NP0353872 (**3**). Genomes for *C. atlanticus* AO-06 and *C. atlanticus* AO-30 have been deposited as Genbank BioSample accessions SAMN56710389 and SAMN56710390 and will be released with publication (https://www.ncbi.nlm.nih.gov/biosample/56710389, https://www.ncbi.nlm.nih.gov/biosample/56710390).

Supporting Information

The Supporting Information is available free of charge at https://pubs.acs.org/doi/10.1021/acs.jnatprod.6c00098.

NMR, MS, and UV–vis spectra of isolated compounds (PDF)

■ AUTHOR INFORMATION

Corresponding Author

Sandra Loesgen − *Department of Chemistry, Whitney Laboratory for Marine Bioscience, University of Florida, St. Augustine, Florida 32080, United States;* orcid.org/0000-0003-1090-564X; Email: sandra.loesgen@ufl.edu

Authors

Erin M. Marshall − *Department of Chemistry, Whitney Laboratory for Marine Bioscience, University of Florida, St. Augustine, Florida 32080, United States*

Chenxi Zhu − *Department of Chemistry, Whitney Laboratory for Marine Bioscience, University of Florida, St. Augustine, Florida 32080, United States*

Lydia Mayhood − *Department of Biology and Department of Neuroscience, Whitney Laboratory for Marine Bioscience, University of Florida, St. Augustine, Florida 32080, United States*

Zain Khalid − *Department of Biology and Department of Neuroscience, Whitney Laboratory for Marine Bioscience, University of Florida, St. Augustine, Florida 32080, United States*

Haoyi Yao − *Department of Geoscience, The Arctic University of Trømso, Trømso 9037, Norway;* Present Address: Department of Geological Sciences, Stockholm University, Stockholm 10691, Sweden

Giuliana Panieri − *Department of Geoscience, The Arctic University of Trømso, Trømso 9037, Norway;* Present Address: CNR, ISP Institute of Polar Science, Campus Scientifico, Università Ca' Foscari Venezia, Mestre 30172, Italy.

José D. D. Cediel-Becerra − *Department of Microbiology and Cell Science, University of Florida, Gainesville, Florida 32611, United States;* orcid.org/0000-0001-6496-2071

Marc G. Chevrette − *Department of Plant Pathology and Wisconsin Institute for Discovery, University of Wisconsin-Madison, Madison, Wisconsin 53706, United States;* orcid.org/0000-0002-7209-0717

James A. Strother − *Department of Biology and Department of Neuroscience, Whitney Laboratory for Marine Bioscience, University of Florida, St. Augustine, Florida 32080, United States;* orcid.org/0000-0001-6871-5561

Complete contact information is available at: https://pubs.acs.org/10.1021/acs.jnatprod.6c00098

Funding

The Norwegian Research Council supported part of our research through the Centre for Arctic Gas Hydrate, Environment and Climate (project number 223259).

Notes

The authors declare no competing financial interest.

■ ACKNOWLEDGMENTS

We thank Steven Giovannoni (OSU) for providing genome-sequenced *C. atlanticus* HTCC2559^T. We wish to thank Sam Xia (UNF), James Rocca (UF, AMRIS) for excellent NMR support. The National High Magnetic Field Laboratory is supported by the National Science Foundation through NSF/DMR-1644779 and DMR-2128556 and the State of Florida. We wish to thank the NIH PDSP Program for testing benzothiazine BPSS2111-2113:C (**2**, PDSP # 76479) and croceithiazole A (**4**, PDSP # 77893). We also acknowledge Amelia Bunnell, Lucas Cathey, and Alaska Miller for help with zebrafish care and Anabel Mendoza for supporting bacterial strain isolation efforts. This work was supported by NSF CH-2020110 (S.L.). S.L. is grateful for UF and UF Whitney Lab Start-Up funds. Partial support for MGC was provided by a Research Starter Grant award from the American Society for Pharmacognosy.

■ REFERENCES

(1) Raja, S. N.; Carr, D. B.; Cohen, M.; Finnerup, N. B.; Flor, H.; Gibson, S.; Keefe, F. J.; Mogil, J. S.; Ringkamp, M.; Sluka, K. A.; Song, X.-J.; Stevens, B.; Sullivan, M. D.; Tutelman, P. R.; Ushida, T.; Vader, K. The Revised International Association for the Study of Pain Definition of Pain: Concepts, Challenges, and Compromises. *Pain* **2020**, *161* (9), 1976–1982.

(2) Goldberg, D. S.; McGee, S. J. Pain as a Global Public Health Priority. *BMC Public Health* **2011**, *11* (1), 770.

(3) Cohen, S. P.; Vase, L.; Hooten, W. M. Chronic Pain: An Update on Burden, Best Practices, and New Advances. *Lancet* **2021**, *397* (10289), 2082–2097.

(4) Dahlhamer, J.; Lucas, J.; Zelaya, C.; Nahin, R.; Mackey, S.; DeBar, L.; Kerns, R.; Von Korff, M.; Porter, L.; Helmick, C. Prevalence of Chronic Pain and High-Impact Chronic Pain Among Adults - United States, 2016. *Morb. Mortal Wkly. Rep.* **2018**, *67* (36), 1001–1006.

(5) Schwartz, E. S.; La, J.-H.; Scheff, N. N.; Davis, B. M.; Albers, K. M.; Gebhart, G. F. TRPV1 and TRPA1 Antagonists Prevent the Transition of Acute to Chronic Inflammation and Pain in Chronic Pancreatitis. *J. Neurosci.* **2013**, *33* (13), 5603–5611.

(6) Eid, S. R.; Crown, E. D.; Moore, E. L.; Liang, H. A.; Choong, K.-C.; Dima, S.; Henze, D. A.; Kane, S. A.; Urban, M. O. HC-030031, a TRPA1 Selective Antagonist, Attenuates Inflammatory- and Neuropathy-Induced Mechanical Hypersensitivity. *Mol. Pain* **2008**, *4*, 48.
(7) Finnerup, N. B.; Nikolajsen, L.; Rice, A. S. C. Transition from Acute to Chronic Pain: A Misleading Concept? *Pain* **2022**, *163* (9), No. e985.
(8) Bunnell, A. A.; Marshall, E. M.; Estes, S. K.; Deadmond, M. C.; Loesgen, S.; Strother, J. A. Embryonic Zebrafish Irritant-Evoked Hyperlocomotion (EZIH) as a High-Throughput Behavioral Model for Nociception. *Behav Brain Res.* **2025**, *485*, No. 115526.
(9) Cho, J.-C.; Giovannoni, S. J. *Croceibacter atlanticus* Gen. Nov., sp. Nov., A Novel Marine Bacterium in the Family Flavobacteriaceae. *Syst. Appl. Microbiol* **2003**, *26* (1), 76−83.
(10) Kang, I.; Kang, D.; Cho, J.-C. Complete Genome Sequence of Bacteriophage P2559Y, a Marine Phage That Infects *Croceibacter atlanticus* HTCC2559. *Mar. Genomics* **2016**, *29*, 35−38.
(11) Bartolek, Z.; Van Creveld, S. G.; Coesel, S.; Cain, K. R.; Schatz, M.; Morales, R.; Virginia Armbrust, E. Flavobacterial Exudates Disrupt Cell Cycle Progression and Metabolism of the Diatom *Thalassiosira pseudonana*. *ISME J.* **2022**, *16* (12), 2741−2751.
(12) Van Tol, H. M.; Amin, S. A.; Armbrust, E. V. Ubiquitous Marine Bacterium Inhibits Diatom Cell Division. *ISME J.* **2017**, *11* (1), 31−42.
(13) Singh, S. K.; Kotakonda, A.; Kapardar, R. K.; Kankipati, H. K.; Sreenivasa Rao, P.; Sankaranarayanan, P. M.; Vetaikorumagan, S. R.; Gundlapally, S. R.; Nagappa, R.; Shivaji, S. Response of Bacterioplankton to Iron Fertilization of the Southern Ocean, Antarctica. *Front Microbiol* **2015**, *6*, 863 DOI: 10.3389/fmicb.2015.00863.
(14) Kang, I.; Kang, D.; Cho, J.-C. Complete Genome Sequence of *Croceibacter* Bacteriophage P2559S. *J. Virol* **2012**, *86* (16), 8912−8913.
(15) Rundla, H. K.; Soni, S.; Teli, S.; Agarwal, S.; Agarwal, L. K. Evolution in the Synthesis of 1,4-Benzothiazines over the Last Decade (2014 to 2024). *RSC Adv.* **2025**, *15* (8), 6122−6146.
(16) Rai, A.; Singh, A. K.; Raj, V.; Saha, S. 1,4-Benzothiazines-A Biologically Attractive Scaffold. *Mini Rev. Med. Chem.* **2017**, *18* (1), 42 DOI: 10.2174/1389557517666170529075556.
(17) Ajani, O. O. Functionalized 1,4-Benzothiazine: A Versatile Scaffold with Diverse Biological Properties. *Arch. Pharm.* **2012**, *345* (11), 841−851.
(18) Wang, D.; Wang, Y.; Ouyang, Y.; Fu, P.; Zhu, W. Cytotoxic *p*-Terphenyls from a Marine-Derived *Nocardiopsis* Species. *J. Nat. Prod.* **2019**, *82* (12), 3504−3508.
(19) Hosokawa, N.; Naganawa, H.; Iinuma, H.; Hamada, M.; Takeuchi, T.; Kanbe, T.; Hori, M. Thiazinotrienomycins, New Ansamycin Group Antibiotics. *J. Antibiot.* **1995**, *48* (6), 471−478.
(20) Raju, R.; Piggott, A. M.; Khalil, Z.; Bernhardt, P. V.; Capon, R. J. Heronamycin A: A New Benzothiazine Ansamycin from an Australian Marine-Derived *Streptomyces* sp. *Tetrahedron Lett.* **2012**, *53* (9), 1063−1065.
(21) Shaaban, K. A.; Wang, X.; Elshahawi, S. I.; Ponomareva, L. V.; Sunkara, M.; Copley, G. C.; Hower, J. C.; Morris, A. J.; Kharel, M. K.; Thorson, J. S. Herbimycins D−F, Ansamycin Analogues from *Streptomyces* sp. RM-7−15. *J. Nat. Prod.* **2013**, *76* (9), 1619−1626.
(22) Wu, Q.; Zhu, H.; Sun, C.; Zhou, L.; Wang, H.; Shi, S.; Tian, X.; Ju, J. Halo- and Thiocarbazomycins from Coral- and Coral Reef Sands-Derived Actinomycetes. *Mar. Drugs* **2022**, *20* (8), 537.
(23) Yi, K.-X.; Xie, Q.-Y.; Ma, Q.-Y.; Yang, L.; Dai, H.-F.; Zhao, Y.-X.; Hao, Y.-E. Diverse Ansamycin Derivatives from the Marine-Derived *Streptomyces* sp. ZYX-F-97 and Their Antibacterial Activities. *Fitoterapia* **2024**, *173*, No. 105814.
(24) Biggins, J. B.; Liu, X.; Feng, Z.; Brady, S. F. Metabolites from the Induced Expression of Cryptic Single Operons Found in the Genome of *Burkholderia pseudomallei*. *J. Am. Chem. Soc.* **2011**, *133* (6), 1638−1641.
(25) McAvoy, A. C.; Threatt, P. H.; Kapcia, J.; Garg, N. Discovery of Homogentisic Acid as a Precursor in Trimethoprim Metabolism and Natural Product Biosynthesis. *ACS Chem. Biol.* **2023**, *18* (4), 711−723.
(26) Zhang, P.; Jia, C.; Lang, J.; Shen, H.; Li, J.; Chen, S.; Liu, L. Leptothiazinones A and B, Two New Benzothiazinones from a Marine-Derived Fungus *Leptosphaerulina chartarum* 3608. *Phytochem Lett.* **2018**, *27*, 55−58.
(27) Wang, M.; Sun, Z.-H.; Chen, Y.-C.; Liu, H.-X.; Li, H.-H.; Tan, G.-H.; Li, S.-N.; Guo, X.-L.; Zhang, W.-M. Cytotoxic Cochlioquinone Derivatives from the Endophytic Fungus *Bipolaris sorokiniana* Derived from *Pogostemon cablin*. *Fitoterapia* **2016**, *110*, 77−82.
(28) Cooray, N. M.; Scheuer, P. J.; Parkanyi, L.; Clardy, J. Shermilamine A: A Pentacyclic Alkaloid from a Tunicate. *J. Org. Chem.* **1988**, *53* (19), 4619−4620.
(29) Carroll, A. R.; Cooray, N. M.; Poiner, A.; Scheuer, P. J. A Second Shermilamine Alkaloid from a Tunicate *Tridemnum* sp. *J. Org. Chem.* **1989**, *54* (17), 4231−4232.
(30) Serov, P.; Vadakkepuliyambatta, S.; Mienert, J.; Patton, H.; Portnov, A.; Silyakova, A.; Panieri, G.; Carroll, M. L.; Carroll, J.; Andreassen, K.; Hubbard, A. Postglacial Response of Arctic Ocean Gas Hydrates to Climatic Amelioration. *Proc. Natl. Acad. Sci. U. S. A.* **2017**, *114* (24), 6215−6220.
(31) Carroll, M. L. CAGE16−5 Cruise Report: ROV-Based Geological and Biological Investigations of Methane Seeps at Prins Karls Forland, Storfjordrenna Pingos and Bjørnøyrenna Craters *CAGE* 2023; Vol. *4* DOI: 10.7557/cage.6928.
(32) Panieri, G.; Alexandropoulou, N.; Bruvik, K. L.; Carrier, V.; Dessandier, P.-A.; Dølven, K. O.; Valberg, E.; Fornari, D.; Gründger, F.; Kurras, G. J.; Yao, H.; Holm, T.; Lindgren, M.; Melaniuk, K.; Olsen, B. R.; Ofstad, S.; Patton, H.; Romeyn, R.; Sauer, S.; Sen, A.; Sert, M. CAGE17−2 Cruise Report: Gas Hydrate Deposits and Methane Seepages in Storfjordrenna, Northern Flank of Olga Basin, and West Sentralbanken (Barents Sea): Biogeochemical and Biological Investigations *CAGE* 2023; Vol. 5 DOI: 10.7557/cage.6955.
(33) Altschul, S. F.; Gish, W.; Miller, W.; Myers, E. W.; Lipman, D. J. Basic Local Alignment Search Tool. *J. Mol. Biol.* **1990**, *215* (3), 403−410.
(34) Eren, A. M.; Esen, Ö. C.; Quince, C.; Vineis, J. H.; Morrison, H. G.; Sogin, M. L.; Delmont, T. O. Anvi'o: An Advanced Analysis and Visualization Platform for 'omics Data. *PeerJ.* **2015**, *3*, No. e1319.
(35) Delmont, T. O.; Eren, A. M. Linking Pangenomes and Metagenomes: The *Prochlorococcus* Metapangenome. *PeerJ* **2018**, *6*, No. e4320.
(36) Williamson, R. T.; Márquez, B. L.; Gerwick, W. H.; Kövér, K. E. One- and Two-dimensional Gradient-selected HSQMBC NMR Experiments for the Efficient Analysis of Long-range Heteronuclear Coupling Constants. *Magn. Reson. Chem.* **2000**, *38* (4), 265−273.
(37) Haney, W. A.; Moussaoui, B.; Strother, J. A. Prolonged Exposure to Stressors Suppresses Exploratory Behavior in Zebrafish Larvae. *J. Exp Biol.* **2020**, *223* (22), No. jeb.224964.
(38) Wiegand, I.; Hilpert, K.; Hancock, R. E. W. Agar and Broth Dilution Methods to Determine the Minimal Inhibitory Concentration (MIC) of Antimicrobial Substances. *Nat. Protoc.* **2008**, *3* (2), 163−175.
(39) CLSI. *Methods for Dilution Antimicrobial Susceptibility Tests for Bacteria That Grow Aerobically*, 11th ed.; Clinical and Laboratory Standards Institute: Wayne, PA, 2018; Vol. CLSI standard M07.
(40) CLSI. *Performance Standards for Antimicrobial Susceptibility Testing*, 30th ed.; CLSI supplement M100; Clinical and Laboratory Standards Institute: Wayne, PA, 2020.
(41) Mosmann, T. Rapid Colorimetric Assay for Cellular Growth and Survival: Application to Proliferation and Cytotoxicity Assays. *J. Immunol Methods* **1983**, *65* (1−2), 55−63.
(42) Besnard, J.; Ruda, G. F.; Setola, V.; Abecassis, K.; Rodriguiz, R. M.; Huang, X.-P.; Norval, S.; Sassano, M. F.; Shin, A. I.; Webster, L. A.; Simeons, F. R. C.; Stojanovski, L.; Prat, A.; Seidah, N. G.; Constam, D. B.; Bickerton, G. R.; Read, K. D.; Wetsel, W. C.; Gilbert, I. H.; Roth, B. L.; Hopkins, A. L. Automated Design of Ligands to Polypharmacological Profiles. *Nature* **2012**, *492* (7428), 215−220.

(43) Kroeze, W. K.; Sassano, M. F.; Huang, X.-P.; Lansu, K.; McCorvy, J. D.; Giguère, P. M.; Sciaky, N.; Roth, B. L. PRESTO-Tango as an Open-Source Resource for Interrogation of the Druggable Human GPCRome. *Nat. Struct. Mol. Biol.* **2015**, *22* (5), 362−369.
(44) Knox, W. E.; LeMay-Knox, M. The Oxidation in Liver of l -Tyrosine to Acetoacetate through *p* -Hydroxyphenylpyruvate and Homogentisic Acid. *Biochem. J.* **1951**, *49* (5), 686−693.
(45) Lindstedt, S.; Odelhog, B.; Rundgren, M. Purification and Some Properties of 4-Hydroxyphenylpyruvate Dioxygenase from *Pseudomonas* sp. P.J. 874. *Biochemistry* **1977**, *16* (15), 3369−3377.
(46) Cediel-Becerra, J. D. D.; Cumsille, A.; Guerra, S.; Ding, Y.; de Crécy-Lagard, V.; Chevrette, M. G. Targeted Genome Mining with GATOR-GC Maps the Evolutionary Landscape of Biosynthetic Diversity. *Nucleic Acids Res.* **2025**, *53* (13), No. gkaf606.
(47) Blin, K.; Shaw, S.; Vader, L.; Szenei, J.; Reitz, Z. L.; Augustijn, H. E.; Cediel-Becerra, J. D. D.; de Crécy-Lagard, V.; Koetsier, R. A.; Williams, S. E.; Cruz-Morales, P.; Wongwas, S.; Segurado Luchsinger, A. E.; Biermann, F.; Korenskaia, A.; Zdouc, M. M.; Meijer, D.; Terlouw, B. R.; van der Hooft, J. J. J.; Ziemert, N.; Helfrich, E. J. N.; Masschelein, J.; Corre, C.; Chevrette, M. G.; van Wezel, G. P.; Medema, M. H.; Weber, T. antiSMASH 8.0: Extended Gene Cluster Detection Capabilities and Analyses of Chemistry, Enzymology, and Regulation. *Nucleic Acids Res.* **2025**, *53* (W1), W32−W38.
(48) Cediel-Becerra, J. D. D.; Chevrette, M. G. Targeted Genome Mining for Natural Product Discovery. In *Methods Enzymol.*; Elsevier, 2025; p S0076687925001624.
(49) Minh, B. Q.; Schmidt, H. A.; Chernomor, O.; Schrempf, D.; Woodhams, M. D.; Von Haeseler, A.; Lanfear, R. Corrigendum to: IQ-TREE 2: New Models and Efficient Methods for Phylogenetic Inference in the Genomic Era. *Mol. Biol. Evol.* **2020**, *37* (8), 2461.
(50) Letunic, I.; Bork, P. Interactive Tree of Life (iTOL) v6: Recent Updates to the Phylogenetic Tree Display and Annotation Tool. *Nucleic Acids Res.* **2024**, *52* (W1), W78−W82.

https://doi.org/10.1021/acs.jnatprod.6c00098
J. Nat. Prod. 2026, 89, 1265−1275